JFE TECHNICAL REPORT
No. 28 (Sep. 2022)

# Operation Guidance Technique of a Blast Furnace Using Data Science (Part 2)

ITO Tomohiko[*1]    TSUBOI Toshiki[*2]    MASUDA Ryousuke[*3]    SHIMAMOTO Hiroyuki[*4]

***Abstract:***

*In blast furnace operation under low percentage of reducing material, which intends to reduce $CO_2$ emission, the furnace condition easily falls into unstable and in the worst case, serious trouble could occur. Therefore, it is important to operate the furnace with recognizing current condition. However, information from conventional sensors or analysis with the models were not still enough. Accordingly, in JFE Steel, the cyber physical system of the blast furnace has been constructed, and the particle size measurement technique of charging coke in real time, the prediction system of pig iron temperature based on blast furnace physical model, and furnace condition detection technique based on inner pressure data, have been developed as a guidance system based on the visualized inner furnace conditions. These techniques contribute to keep continuous stable operation by presenting the guidance to the operator.*

## 1. Introduction

The blast furnace is a process in which molten pig iron is produced by alternately charging coke and iron ore from the top of the furnace while blowing blast from tuyeres arranged around the furnace hearth, and reducing the iron ore with the carbon in the coke. In the future, reduction of the reducing agent ratio will be required, as this is an effective means of reducing $CO_2$ emissions.

The term "reducing agent" refers to the coke charged from the furnace top and pulverized coal injected from the tuyeres. The amount of reducing agents used in the production of 1 ton of pig iron in a blast furnace is called the reducing agent ratio (RAR); similarly, the amount of coke used in the production of 1 ton of pig iron is called the coke rate. Coke functions as a spacer in the blast furnace, securing the upward flow of the high temperature gas injected from the tuyeres in the blast furnace hearth, and also accelerates the reduction of iron ore by the heat generation accompanying the reduction reaction, thereby facilitating the discharge of pig iron and slag from the furnace.

JFE Steel has applied a cyber-physical system (CPS) to its blast furnaces to maintain high efficiency operation of the BFs under low RAR operation and avoid serious operational trouble. In blast furnace CPS, the sensor data acquired from the actual blast furnace are collected and analyzed, and a virtual blast furnace modeled on these data is implemented in cyberspace in real time. Introduction of the virtual blast furnace has made it possible to understand the state of operation in the blast furnace, which cannot be observed directly, and predict its future state. In addition to enabling stable operation by feeding back the results of monitoring of blast furnace soundness and anomaly predictions to operational actions for the actual blast furnace, blast furnace CPS can also be expected to improve productivity by identification of process bottlenecks (**Fig. 1**).

Recently, JFE Steel has developed more advanced versions of the coke particle size meter for measurement of the coke particle size before charging, operation guidance based on hot metal temperature predic-

† Originally published in *JFE GIHO* No. 49 (Feb. 2022), p. 36–41

[*1] Senior Researcher Deputy General Manager,
Cyber-Physical System Research & Development Dept.,
Steel Res. Lab.,
JFE Steel

[*2] Senior Researcher Deputy Manager,
Cyber-Physical System Research & Development Dept.,
Steel Res. Lab.,
JFE Steel

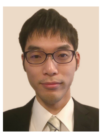

[*3] Senior Researcher Assistant Manager,
Cyber-Physical System Research & Development Dept.,
Steel Res. Lab.,
JFE Steel

[*4] Senior Researcher Manager,
Cyber-Physical System Research & Development Dept.,
Steel Res. Lab.,
JFE Steel

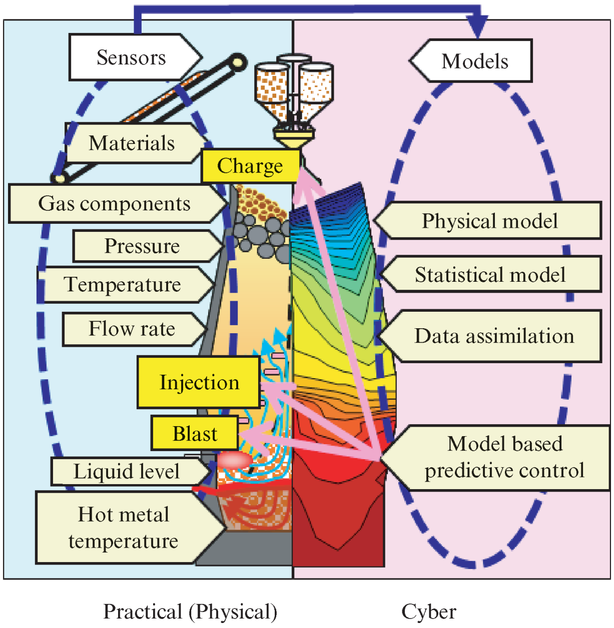


Fig. 1 Schematic diagram of CPS blast furnace

tion, and permeability anomaly detection described in our previous report[1], and these technologies now form the basis of the JFE Steel CPS blast furnace. This paper focuses on the further development and advancement of these technologies.

## 2. Coke Particle Size Meter

The coke charged into a blast furnace includes various particle sizes, but if the ratio of small coke is excessive, the furnace condition will become unstable due to constriction of the gas flow paths between the burden materials. Conventionally, an offline size analysis by sieving (sieve analysis) of coke sampled at the blast furnace had been performed once or twice a week in order to control the tendency of the particle size distribution of the charged coke. However, because the particle size of coke fluctuates with a shorter cycle, action to prevent deterioration of the furnace condition can be taken in advance if increases in the percentage of small coke can be detected at an early timing. Therefore, JFE Steel developed a coke particle size meter which makes it possible to monitor the particle size distribution in real time.

In our previous report[1], we showed that rough agreement between the tendencies of the measured particle size distribution and the distribution obtained by sieving analysis is possible by applying a particle size measurement algorithm using a laser range finder and a particle size distribution correction technique. However, powdery coke (called coke fines) with a particle size of less than 5 mm (-5 mm) adheres to the surface of coarser coke particles by way of moisture, making it difficult to measure the powder ratio by the conventional laser range finder technique. Therefore, based on the physical phenomenon that adhering powder adheres by way of moisture, we devised a new technique using the luminance of camera images (image brightness), which is capable of measuring the powder ratio. By using a hybrid sensor configuration, in which a camera is added to the conventional laser range finder, it is now possible to calculate the particle size distribution of the entire particle size range.

### 2.1 Outline of Coke Particle Size Distribution Meter

The sensor configuration and measurement flow of the particle size distribution meter are shown in **Fig. 2**. As mentioned above, the coke particle size distribution meter has a hybrid sensor configuration consisting of a laser range finder and a camera. The laser range finder is used to capture the surface profile of the coke on the conveyer. The particles in the profile are then detected by image processing, and the particle sizes of the coarse coke in each size range are calculated[1]. Assuming that the coke is spherical and its density is uniform, the particle size distribution, which is the weight percentage for each particle size, is calculated from each coarse coke weight calculated based on the particle size. The weight percentage of -5 mm powder in the particle size distribution is defined as the powder ratio. How-

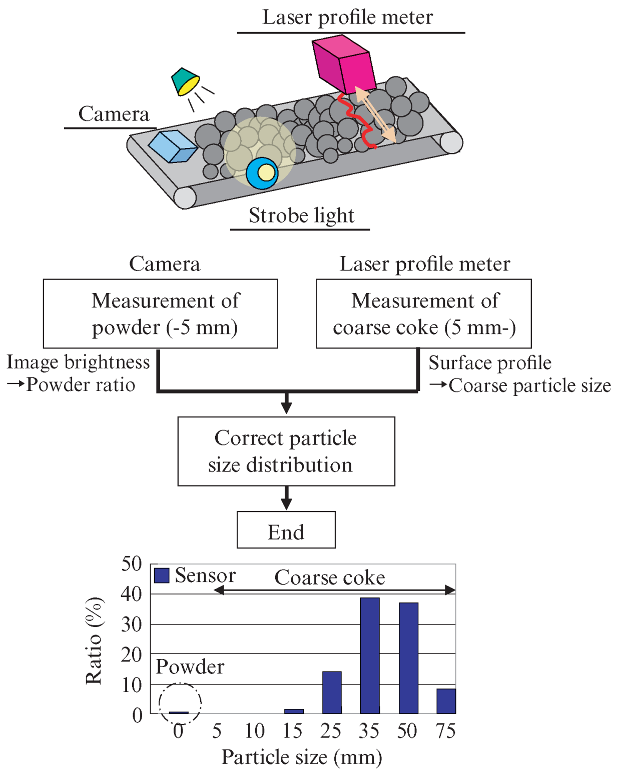


Fig. 2 Sensor configuration and measurement flow of particle size distribution of coke

ever, since there is a limit to the optical resolution of the laser range finder, the adhering powder was too small to measure with only the laser device. On the other hand, the resolution of the camera alone is also inadequate. Therefore, this problem was solved by estimation processing using the camera luminance, as described below. Calculation of the particle size distribution of the entire particle size range was made possible by combining the information of these two sensors and correcting the particles size distribution statistically[1].

### 2.2 Principle of Powder Ratio Measurement

The new measurement technique using camera luminance was devised based on the physical phenomenon that the adhering powder adheres via moisture. **Figure 3** shows the principle of measurement of the powder ratio of coke. Here, ① represents the relationship between the powder ratio and the moisture content of the coke obtained by manual analysis. The moisture content is calculated by the dry analysis method specified in the JIS method. As shown in ①, if the moisture content of the coke increases, the powder ratio also increases. This expresses the fact that the powder adheres more easily as the moisture content of the coke increases. ② shows camera images of the measurement of the coke surface in the case of coke moisture contents of 2 % and 10 %. It can be understood that the luminance of the image decreases when the moisture content of the coke increases. Generally, there are two types of light reflection from objects, a diffuse reflection component and a specular reflection component. The diffusion reflection component is light which is scattered uniformly in all directions by the reflecting surface, while the specular reflection component is the light resulting from strong reflection of incident light in a specific direction. When the moisture content increases, it is known that the specular reflection component becomes stronger at surfaces where the surface of the object is covered with water, and conversely, the diffuse reflection component becomes weaker[2]. Since the camera primarily captures the diffuse reflection component, it is thought that image luminance, which is mainly caused by the diffuse light component, will decrease if the moisture content increases.

Using the relationship of the above-mentioned two types of reflected light, the powder ratio was estimated from the coke images captured by the strobe light and camera system.

### 2.3 Online Actual Machine Test

In order to verify the measurement principle using coke charged at an actual blast furnace, a camera was installed at the coke conveyor of West Japan Works (Kurashiki District) No. 3 blast furnace, and an actual machine test was conducted. For comparison, the moisture content values of the existing neutron moisture meter were also collected, considering the possibility that the powder can be measured by way of the moisture content. Here, the neutron moisture meter is a device in which neutrons irradiated from a neutron source are partially transmitted through the coke in the raw material hopper and are reflected corresponding to the moisture content, the reflected neutrons are detected by a detector, and the moisture content is then calculated from the amount of reflected neutrons.

**Figure 4** (a) shows the relationship between the powder ratio obtained by sieve analysis and measurement camera luminance, and (b) shows the relationship between the powder ratio and the moisture content values obtained with the neutron moisture meter. As shown in Fig. 4 (a), it was found that the powder ratio can be measured in real time from image luminance with a coefficient of determination of the powder ratio and luminance of $R^2 = 0.61$ and a standard deviation of error of $\sigma = 0.15$ %. The error of the primary evaluation data during the test period relative to the fluctuation of the powder ratio obtained by sieve analysis during normal operation was quite small, confirming that the camera luminance technique has sufficient

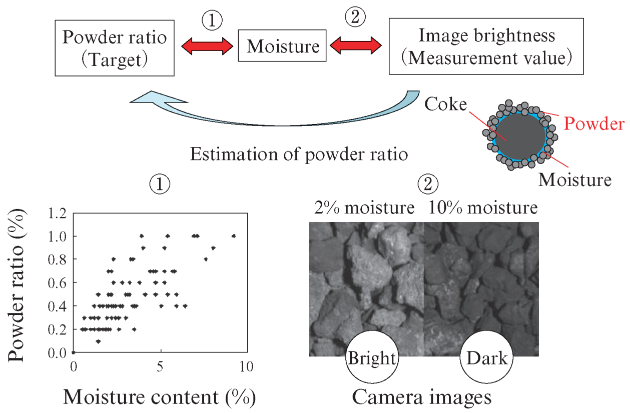


Fig. 3 Measurement principle of powder ratio of coke

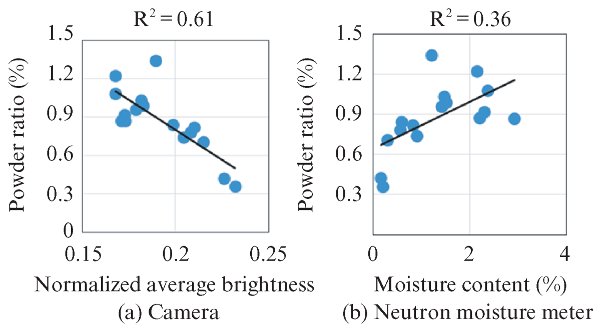


Fig. 4 Correlation between powder ratio and each index

accuracy for application to blast furnace operation.

As shown in Fig. 4 (b), measurement with a coefficient of determination $R^2 = 0.36$ and standard deviation of error $\sigma = 0.20$ % was also possible by using the neutron moisture meter, but accuracy was higher with the technique using camera luminance. Considering the phenomenon that powder adheres via moisture, a technique based on surface moisture is considered to be suitable for measurement of the powder ratio, since the moisture which contributes to powder adhesion is surface moisture, and not the moisture content in the interior of the coke. According to the principle of the neutron moisture meter, neutrons permeate through the coke, which means that the meter measures internal moisture in addition to surface moisture. In contrast, because the camera captures the reflection of visible light, camera luminance is only sensitive to the moisture on the coke surface. For this reason, it is thought that camera luminance has higher estimation accuracy for the powder ratio.

As described above, it has become possible to grasp the particle size distribution of the entire particle size range by adding a camera for measurement of the powder ratio, and as a result, even more appropriate blast furnace operation is now possible.

## 3. Guidance System for Hot Metal Temperature Control

JFE Steel implemented an operation guidance system based on hot metal temperature prediction 8 hours in advance by a physical model of the blast furnace, and has introduced and uses this system at all blast furnaces operated by the company[3]. This chapter describes the creation of a model simulating the operational actions taken by operators to keep a constant hot metal temperature, and the further reduction of variations in the hot metal temperature achieved by incorporating this model in the guidance system for hot metal temperature control[4].

### 3.1 Problem and Approach of Guidance System for Hot Metal Temperature Control

The physical model using by the guidance system for hot metal temperature control described in the literature[3] had the problem of reduced control performance in case of external disturbances that are difficult to express by a physical model, such as variations in the burden descent rate, etc. However, even under poor operating conditions, experienced operators can take appropriate operational actions based on sensor information such as the top gas temperature and tuyere temperature. Therefore, an operator behavior model was constructed by modeling the operational actions themselves which operators take for hot metal temperature (HMT) control.

Since operators take operational actions by visually grasping the trends of process variables, in this model, we used a convolutional neural network (CNN), which is widely used in the field of image processing.

### 3.2 Construction of Operator Behavior Model

**Table 1** shows the main process variables which operators consider when deciding HMT control actions. Among these variables, the loading rate means the number of charges of burden materials charged from the top of the blast furnace per hour and is an index that expresses the burden descent rate. Because the iron ore will reach the hearth without being completely reduced if the loading rate is excessive, there is an increased possibility of a decrease in HMT. The tuyere temperature is defined as the average of the temperature measurement values obtained by thermocouples embedded in approximately 40 tuyeres installed around the furnace hearth. Since the tuyere temperature is influenced by radiation from the coke bed and the hot metal, this variable tends to change ahead of HMT.

Operators monitor the trends in the main process variables, tracing back a point about 1 day before the present time, in order to understand the degree of effect of operational actions taken in the past on HMT and the process variables that have a high correlation with HMT. The operators also predict future changes in HMT from the trends in the main process variables in the most recent several hours in order to take appropriate operational action.

In the operator behavior model, information in connection with the main process variables is input. A 2-dimensional matrix was prepared by standardizing and arranging the data for each process variable in the most recent 32 hours, using the 30 minute average values of the operational data.

Because the control inputs decided by operators per one operation are substantially uniform, the model does not make quantitative predictions of control inputs, and only outputs the direction (increase, decrease, hold) of the control actions by operators.

Table 1 Process variables that operators consider important

| No. | Variable | Unit |
|---|---|---|
| 1 | Control error of hot metal temperature (HMT) | °C |
| 2 | Coke rate | kg/t |
| 3 | Top gas temperature | °C |
| 4 | Loading rate | ch/hour |
| 5 | Tuyere temperature | °C |

Therefore, the three levels of “Increase HMT,” “Decrease HMT” and “Hold” (i.e., monitor conditions without taking action) were given to the respective data. However, cases that were judged to be erroneous control actions were excluded from the training data in advance to prevent simulation of erroneous actions by operators[4].

Next, the prepared matrix was input to the CNN as an image in which the abscissa represents time and the ordinate shows the data items. The CNN comprises three layers, a convolution layer, a pooling layer and a fully connected layer. In the convolution layer, convolution operations are performed by a filter, which is a rectangular weight matrix, and activation is performed by a nonlinear function. In this research, convolution operations are executed only for the temporal axis, and a ReLU (Rectified Linear Unit) was adopted as the activation function[5]. Downsampling is performed in the pooling layer. Weighting is done in the fully connected layer, and the probabilities of the three classes of Increase HMT, Decrease HMT and Hold are output by a Softmax function. **Table 2** shows the network architecture of the CNN, where Conv, Pool and Fc mean convolution layer, pooling layer and fully connected layer, respectively. All layers are connected in series.

In the operator behavior model, the value obtained by subtracting the probability of a Decrease HMT action from the probability of an Increase HMT action is defined as the predicted action value. Cases where the predicted action value exceeds the upper threshold were defined as Increase HMT action judgments, while cases where the value is lower than the lower threshold were defined as Decrease HMT action judgments.

### 3.3 Result of Validation Using Actual Operational Data

The preprocessing described in the previous section was done for the operational data from 2019 at West Japan Work (Kurashiki District) No. 2 blast furnace, and 6 000 datapoints were prepared for each 30 minutes. The initial 5 400 points were used as the training data, 300 points were used as validation data for tuning the hyperparameters of the CNN, and the remaining 300 point were used as the test data for evaluation of the predictive performance of the operator behavior model.

**Figure 5** shows the results of validation of the operator behavior model. The red line in Fig. 5 represents the predicted action values output by the operator behavior model, and the blue plots mean actions that were actually executed by operators. The tendencies of the actions taken by the operators and the predicted action values output by the operator behavior model were generally in agreement.

**Table 3** shows a confusion matrix summarizing the classification of Increase HMT judgments, Decrease HMT judgments and Hold judgments by the operator behavior model. The green lines in Fig. 5 are the upper and lower threshold values. The threshold values were determined so that the ratios of the actual actions and the predicted actions were the same for all test data. The agreement rate between the judgments by the operator behavior model and the actual actions was 57.3 %, while the ratio of cases where the judgment by the operator behavior model and the actual actions had opposite directions was <1 %, showing satisfactory predictive accuracy.

### 3.4 Result of Evaluation in Actual Operation

The operator behavior model developed in this study was incorporated in the guidance system for hot metal temperature control based on model-based predictive control by a physical model in the previous report. **Table 4** shows the relationship between the con-

Table 2 Network architecture of CNN

| Layer | Patch size | Stride | Output feature map size | Activation function |
|---|---|---|---|---|
| Data | | | 64 × 5 | |
| Conv1 | 5 × 1 | 1 | 60 × 5 | ReLU |
| Pool | 2 × 1 | 2 | 30 × 5 | |
| Fc1 | | | 1 × 2 | ReLU |
| Fc2 | | | 1 × 3 | Softmax |

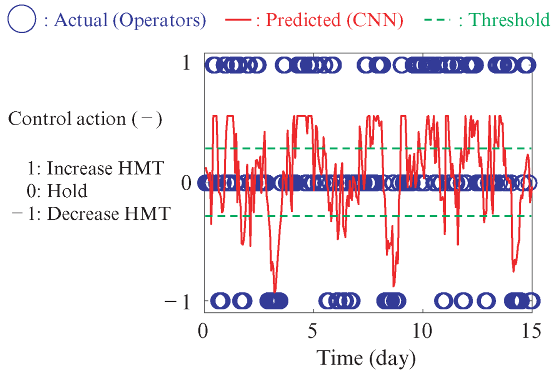


Fig. 5 Comparison between actual and predicted actions

Table 3 Confusion matrix of operator model

| | | Predicted action by CNN | | |
|---|---|---|---|---|
| | | Up | Stay | Down |
| Actual action by operators | Up | 20.7 % | 18.7 % | 0.3 % |
| | Stay | 12.0 % | 22.7 % | 7.0 % |
| | Down | 0.7 % | 4.0 % | 14.0 % |

Table 4 Recommended control action by the guidance system

| | | Transient model-based control | | |
|---|---|---|---|---|
| | | Increase | Hold | Decrease |
| Operator model-based control | Increase | Increase | Increase | Hold |
| | Hold | Increase | Hold | Decrease |
| | Decrease | Hold | Decrease | Decrease |

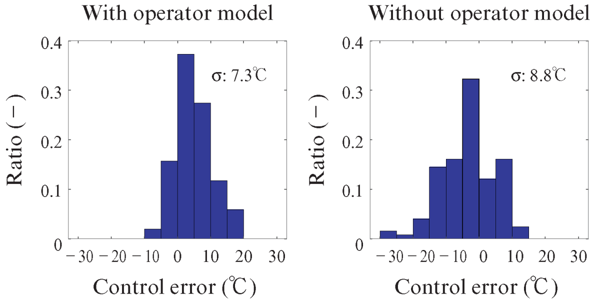


Fig. 6 Control accuracy of hot metal temperature

trol action output by the physical model, the control action output by the operator behavior model and the recommended action, which is the final output of the guidance system. As can be seen in Table 4, when the control action by the physical model and the control action by the operator behavior model have opposite directions, the recommended action is Hold.

A long-term operation test of the operation guidance system based on hot metal temperature prediction including the operator behavior model was carried at West Japan Works Kurashiki No. 2 blast furnace. **Figure 6** shows the results of an evaluation of control accuracy of the hot metal temperature with and without the operator behavior model. The root mean square $\sigma$ of HMT control deviation by the guidance system with the operator model decreased by 1.5°C in comparison with the conventional guidance system without the operator behavior model. Thus, it can be said that the introduction of the operator behavior model improved the effectiveness of guidance system in reducing HMT variations. The operation guidance system based on hot metal temperature prediction incorporating the operator behavior model is now used in the standard production process at multiple blast furnaces operated by JFE Steel.

## 4. Permeability Anomaly Guidance

Under blast furnace operation aiming for low RAR of recent years, there is an increased possibility of decreased permeability in the furnace, and with a further deterioration in permeability, there is also a higher likelihood of the trouble called "channeling," in which the upward flow of the ascending blast is locally concentrated. Since even small channeling trouble can cause collapse of the burden in the furnace and may become a cause of serious trouble in the longer term, it is desirable to take action in advance, for example, by reducing the blast volume. However, it is not necessarily possible to recognize anomalies that may lead to channeling in the future with only the conventional method of setting a threshold for ventilating resistance and monitoring the furnace condition. In such cases, the operator may be slow to realize that an anomaly exists, or overlook an anomaly entirely.

JFE Steel developed a permeability anomaly detection technique and guidance system utilizing Q statistics, which is a multivariate statistical process control (MSPC) technique[1]. In this system, the data groups obtained by pressure gauges that were already installed in the shaft surface layer in the circumferential and height directions are used as the input [1, 6].

**Figure 7** shows the temporal change in the furnace pressure data obtained from the shaft pressure gauge. In the previously-developed anomaly detection technique, disturbances in the synchronicity of multiple shaft pressure values, as shown in Fig. 7, which indicate deterioration of permeability, were indexed as a single value by the Q statistics technique, and a threshold was set for that value and used in judging anomalies.

### 4.1 Detection of Anomaly Signs by Q Statistics

Anomaly detection based on a threshold value of the Q statistic makes it possible to detect conditions where comparatively large variations exist in the shaft pressure values, for example, before channeling occurs. However, if "signs" with smaller variations can be captured, it is assumed that trouble can be minimized. Therefore, we developed a sign detection technique using the count-up method to capture the signs of anomalies using Q statistics. **Figure 8** shows the anomaly detection method using Q statistics.

### 4.2 Example of Sign Detection by Q Statistics

The possibility of capturing the signs of all trouble

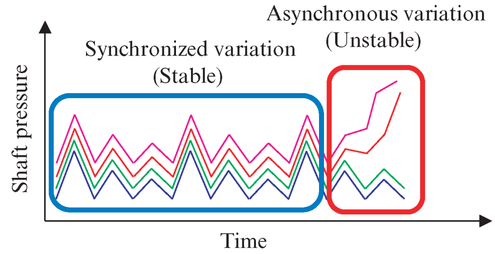


Fig. 7 Shaft pressure change in normal/anomaly operation

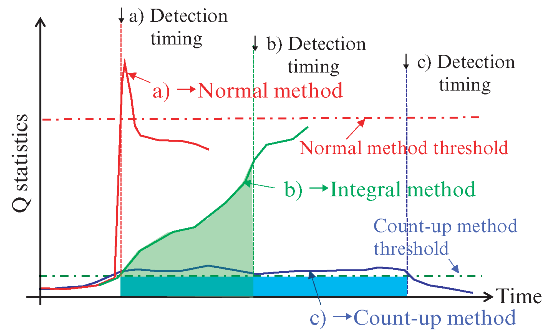


Fig. 8 Anomaly detection methods using Q statistics

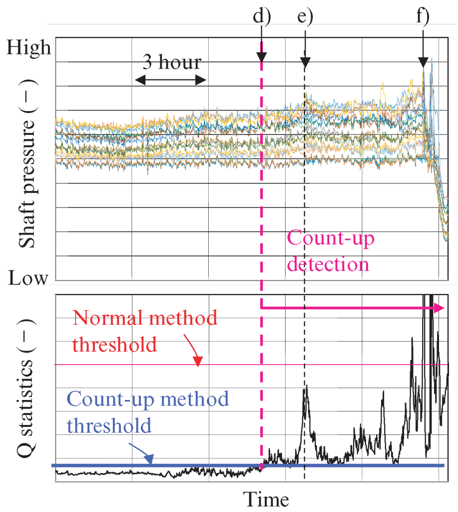


Fig. 9 Example of anomaly prediction using Q statistics

that occurred in a blast furnace in the past 3 years by any of the three techniques described above was investigated. As one example, **Fig. 9** shows the result of an off-line validation of anomaly sign detection by the count-up method for cases where large fluctuation actually occurred in the shaft pressure. The upper part of Fig. 9 shows the trend data for the shaft pressure, and the lower part shows the Q statistic trend. When the fluctuation of the shaft pressure became gradually larger, the level of the Q statistic also increased and exceeded the count-up threshold. After the Q statistic exceeded the threshold value, a sign of an anomaly was detected at the timing indicated by d) in the figure after the passage of a set time of 15 minutes, after which that detection of the anomaly sign continued. Subsequently, the shaft pressure fluctuation became gradually larger (Fig. 9 (e)), and the Q statistic increased further while continuing to exceed the threshold. The shaft pressure fluctuation then became large at the timing of f) in the figure, leading to a reduction of the blast volume.

In this example, it was possible to capture the "sign" of a blast furnace anomaly by the count-up method approximately 6 hours before the actual trouble occurred. Anomaly detection by the previously-developed Q statistic technique (Fig. 8 a)) was 24 minutes earlier. In actual operation, the operator is given guidance to take action to reduce the volume of blast blown into the furnace through the tuyeres if a sign of an anomaly is detected by any of the three techniques shown in Fig. 8. This guidance system is currently in actual operation at all JFE Steel blast furnaces.

## 5. Conclusion

As described above, the level of the CPS blast furnace was enhanced by developing an advanced coke particle size meter, hot metal temperature control technology and permeability anomaly guidance. As a result of the introduction of these technologies, further improvements in blast furnace operation efficiency and stability can be foreseen. The authors also plan to continuously improve the functions of the blast furnace CPS in the future.

## References


1) Ito, T.; Hashimoto, Y.; Shimamoto, H. Operation Guidance Technique of Blast Furnace Using Data Science. JFE Technical Report. 2021, no. 26, p. 21–27.
2) Color Science Association of Japan. Handbook of Color Science. second ed., Tokyo university Press, 1984, p. 222 (in Japanese).
3) Hashimoto, Y.; Okamoto, Y.; Kaise, T.; Sawa, Y. Practical operation guidance on thermal control of blast furnace. ISIJ Int., 2019, vol. 59, p. 1573–1581.
4) Hashimoto, Y.; Masuda, R.; Yasuhara, S. An operator behavior model for thermal control of blast furnace. ISIJ Int., 2022, vol. 62, no. 1, p. 157–164.
5) Nair, V.; Hinton, G. E. Rectified linear units improve restricted boltzmann machines. Proceedings of the 27-th international conference on machine learning (ICML-10) . 2010, p. 807.
6) Shimamoto, H.; Ito, T.; Nishimura, N.; Yamaguchi, T. Abnormality detection of shaft pressures in the blast furnace using Q statistic. Current advances in materials and processes, report of the ISIJ meeting. 2018, vol. 31, no. 2, p. 706.